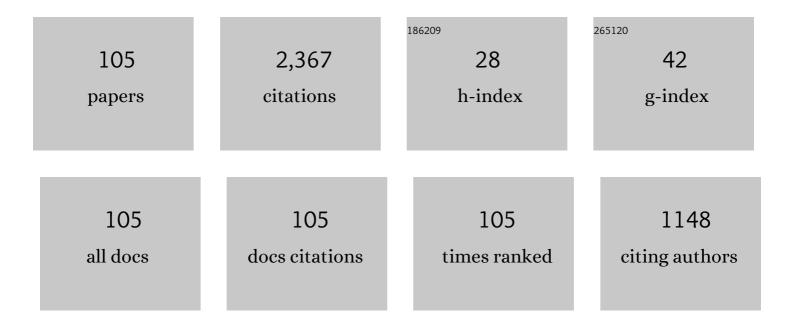
List of Publications by Year in descending order

Source: https://exaly.com/author-pdf/2274932/publications.pdf Version: 2024-02-01



#	Article	IF	CITATIONS
1	Investigation of microstructure and wear resistance of laser-clad CoCrNiTi and CrFeNiTi medium-entropy alloy coatings on Ti sheet. Optics and Laser Technology, 2022, 145, 107518.	2.2	47
2	Effects of β-cooling rates on microstructural characteristics and hardness of Ti–5Al–5Mo–5V–3Cr–1Fe metastable β Ti alloy. Materials Chemistry and Physics, 2022, 276, 125318.	2.0	11
3	Temperature and Stress Field Analysis for Pulsed Laser-Cladding of Pure Titanium on Ti-6Al-4V. Jom, 2022, 74, 755-763.	0.9	4
4	Laser-clad Nb(Ta)TiZr medium-entropy alloy coatings on pure Zr sheet: Microstructural characteristics, hardness and wear resistance. Intermetallics, 2022, 143, 107498.	1.8	11
5	Microstructure, Texture, and Hardness Evolution of Cold-Rolled High-Purity Ti Sheet During Annealing at 350 °C to 550 °C. Metallurgical and Materials Transactions A: Physical Metallurgy and Materials Science, 2022, 53, 2086-2098.	1.1	3
6	Effects of pulsed laser surface remelting on microstructure, hardness and lead-bismuth corrosion behavior of a ferrite/martensitic steel. Nuclear Engineering and Technology, 2022, 54, 1972-1981.	1.1	9
7	Redistribution and refinement of the dendrites in a Mg-Y alloy by laser surface remelting and its influence on mechanical properties. Materials Science & Engineering A: Structural Materials: Properties, Microstructure and Processing, 2022, 848, 143362.	2.6	2
8	Revealing Microstructural, Textural, and Hardness Evolution of Ti–6Al–4V Sheet Cooled From Sub β-Transus Temperature at Different Rates. Metallurgical and Materials Transactions A: Physical Metallurgy and Materials Science, 2022, 53, 3179-3193.	1.1	10
9	Influence of Initial Textures on Microstructure and Mechanical Properties of Commercially Pure TA2 Titanium Sheet Pre-Strained by Cryorolling. Metals and Materials International, 2021, 27, 717-724.	1.8	1
10	Microstructural and textural differences between rolled Zr702 and Zr-2.5Nb alloys: The role played by preexisting β phase. Materials Chemistry and Physics, 2021, 259, 124026.	2.0	2
11	Effects of Î ² Air Cooling and Subsequent Cold Rolling on Microstructure and Hardness of Zr702 Sheet. Metals and Materials International, 2021, 27, 384-391.	1.8	2
12	Editorial: Hexagonal Close-Packed Metals and Alloys: Processing, Microstructure and Properties. Frontiers in Materials, 2021, 8, .	1.2	0
13	A strategy to introduce gradient equiaxed grains into Zr sheet by combining laser surface treatment, rolling and annealing. Scripta Materialia, 2021, 196, 113761.	2.6	12
14	Microstructure and hardness of NbTiZr and NbTaTiZr refractory medium-entropy alloy coatings on Zr alloy by laser cladding. Applied Surface Science, 2021, 549, 149338.	3.1	44
15	Microstructure and properties of pure titanium coating on Ti-6Al-4V alloy by laser cladding. Surface and Coatings Technology, 2021, 416, 127137.	2.2	37
16	Microstructural characteristics, hardness and wear resistance of a typical ferritic/martensitic steel surface-treated by pulsed laser. Surface and Coatings Technology, 2021, 418, 127261.	2.2	14
17	Microstructure and electronic structure of Cr2C and Fe2Y in the Cr-coating prepared by pack-cementation on the surface of ODS steel. Materials Today Communications, 2021, 28, 102591.	0.9	2
18	Microstructure and wear properties of laser-clad NiCo alloy coating on Inconel 718 alloy. Journal of Alloys and Compounds, 2021, 879, 160412.	2.8	20

#	Article	IF	CITATIONS
19	Effects of β-cooling rates on microstructural characteristics and hardness variation of a dual-phase Zr alloy. International Journal of Refractory Metals and Hard Materials, 2021, 100, 105619.	1.7	8
20	Process parameter optimization and anisotropy sensitivity study for abrasive belt grinding of nickel-based single-crystal superalloy. Archives of Civil and Mechanical Engineering, 2021, 21, 1.	1.9	8
21	Quantitative study of microstructural, textural and hardness evolution of high-purity Ti sheet during rolling from low to medium strains. Materials Today Communications, 2021, 29, 102989.	0.9	6
22	Phase constitution, microstructure and properties of pulsed laser-clad ternary CrNiTi medium-entropy alloy coating on pure titanium. Surface and Coatings Technology, 2020, 402, 126503.	2.2	35
23	Microstructural characteristics and hardness of CoNiTi medium-entropy alloy coating on pure Ti substrate prepared by pulsed laser cladding. Journal of Alloys and Compounds, 2020, 849, 156704.	2.8	39
24	Dataset for microstructure and mechanical properties of (CrCoNi)97Al1.5Ti1.5 medium entropy alloy twisted by free-end-torsion at room and cryogenic temperatures. Data in Brief, 2020, 33, 106333.	0.5	1
25	Effect of Heterogeneous Surface Structure on Mechanical Properties of Interstitial-Free Steel Subjected to Laser Surface Treatment. Journal of Materials Engineering and Performance, 2020, 29, 6831-6839.	1.2	0
26	Microstructure and mechanical properties of (CrCoNi)97Al1.5Ti1.5 medium entropy alloy twisted by free-end-torsion at room and cryogenic temperatures. Materials Science & Engineering A: Structural Materials: Properties, Microstructure and Processing, 2020, 797, 140101.	2.6	10
27	Typical Microstructural Characteristics of Ti–5Al–5Mo–5V–3Cr–1Fe Metastable β Ti Alloy Forged in α Region. Acta Metallurgica Sinica (English Letters), 2020, 33, 1601-1608.	+â€9	‰j²
28	Influence of \$\${delta^{prime}}\$\$ Phase with GP-I Zones Fillings on Slip Behavior and Cold Rolling Texture in AA2099. Metals and Materials International, 2020, 27, 3307.	1.8	2
29	Surface microstructural characteristics and hardness of Cr-coated Zr702 sheet processed by pulsed laser. Intermetallics, 2020, 119, 106710.	1.8	7
30	Characterization and correlation of microstructure and hardness of Ti–6Al–4V sheet surface-treated by pulsed laser. Journal of Alloys and Compounds, 2020, 826, 154243.	2.8	24
31	Correlation of microstructural, textural characteristics and hardness of Ti–6Al–4V sheet β-cooled at different rates. Journal of Materials Science, 2020, 55, 8346-8362.	1.7	38
32	Microstructural characteristics and properties of CoCrFeNiNbx high-entropy alloy coatings on pure titanium substrate by pulsed laser cladding. Applied Surface Science, 2020, 517, 146214.	3.1	101
33	Effects of pulsed laser surface treatments on microstructural characteristics and hardness of CrCoNi medium-entropy alloy. Philosophical Magazine, 2019, 99, 3015-3031.	0.7	14
34	Intensified texture of Zr702 sheet after slow cooling from near Î ² -transus temperature. Materials Science and Technology, 2019, 35, 1822-1830.	0.8	0
35	Mis-layered structure of twin-twin interface with 7.4°<-12-10> misorientation relationship in Mg alloy. Materials Science & Engineering A: Structural Materials: Properties, Microstructure and Processing, 2019, 763, 138115.	2.6	5
36	Influence of Torsion on Precipitation and Hardening Effects during Aging of an Extruded AZ91 Alloy. Journal of Materials Engineering and Performance, 2019, 28, 4403-4414.	1.2	6

#	Article	IF	CITATIONS
37	Regulating Precipitates by Simple Cold Deformations to Strengthen Mg Alloys: A Review. Materials, 2019, 12, 2507.	1.3	18
38	Misorientation characteristics and textural changes induced by dense twins in high-purity Ti sheet after small strain rolling. Science China Technological Sciences, 2019, 62, 1968-1975.	2.0	10
39	Effect of Electropulsing Treatment on Microstructure and Mechanical Properties of a Deformed ZrTiAlV Alloy. Materials, 2019, 12, 3560.	1.3	10
40	Influences of Laser Surface Alloying with Cr on Microstructural Characteristics and Hardness of Pure Ti. Metallurgical and Materials Transactions A: Physical Metallurgy and Materials Science, 2019, 50, 3794-3804.	1.1	15
41	Texture control by {10-12} twinning to improve the formability of Mg alloys: A review. Journal of Materials Science and Technology, 2019, 35, 2269-2282.	5.6	79
42	High thermal stability and excellent mechanical properties of ultrafine-grained high-purity copper sheets subjected to asymmetric cryorolling. Materials Characterization, 2019, 153, 34-45.	1.9	33
43	Effect of Shear Strain Rate on Microstructure and Properties of Austenitic Steel Processed by Cyclic Forward/Reverse Torsion. Materials, 2019, 12, 506.	1.3	9
44	Effect of heterogeneous laser surface treatment on mechanical properties of interstitial free steel. IOP Conference Series: Materials Science and Engineering, 2019, 580, 012029.	0.3	1
45	Comparative Study of Microstructural Characteristics and Hardness of β-Quenched Zr702 and Zr–2.5Nb Alloys. Materials, 2019, 12, 3752.	1.3	3
46	Microstructure, texture evolution and mechanical properties of pure Ti by friction stir processing with slow rotation speed. Materials Characterization, 2019, 148, 1-8.	1.9	26
47	Ultra-fine grain size and exceptionally high strength in dilute Mg–Ca alloys achieved by conventional one-step extrusion. Materials Letters, 2019, 237, 65-68.	1.3	58
48	Effects of laser surface alloying with Cr on microstructure and hardness of commercial purity Zr. Journal of Alloys and Compounds, 2019, 784, 1106-1112.	2.8	36
49	Development of Grain Boundary Character Distribution in Medium-Strained 316L Stainless Steel During Annealing. Metals and Materials International, 2019, 25, 364-371.	1.8	16
50	Development of low-alloyed and rare-earth-free magnesium alloys having ultra-high strength. Acta Materialia, 2018, 149, 350-363.	3.8	287
51	Microstructural characterization and hardness variation of pure Ti surface-treated by pulsed laser. Journal of Alloys and Compounds, 2018, 741, 116-122.	2.8	45
52	Strengthening and toughening austenitic steel by introducing gradient martensite via cyclic forward/reverse torsion. Materials and Design, 2018, 143, 150-159.	3.3	36
53	Corrosion behavior of non-equilibrium Zr-Sn-Nb-Fe-Cu-O alloys in high-temperature 0.01â€ [−] M LiOH aqueous solution and degradation of the surface oxide films. Corrosion Science, 2018, 136, 221-230.	3.0	41
54	Nanotwins induced by pulsed laser and their hardening effect in a Zr alloy. Journal of Alloys and Compounds, 2018, 748, 163-170.	2.8	50

LIN JIANG CHAI

#	Article	IF	CITATIONS
55	Strengthening or weakening texture intensity of Zr alloy by modifying cooling rates from αÂ+ β region. Materials Chemistry and Physics, 2018, 213, 414-421.	2.0	18
56	Microstructural characteristics of cold-rolled Zr-2.5Nb alloy annealed near the monotectoid temperature. Science China Technological Sciences, 2018, 61, 558-566.	2.0	7
57	Microstructural and Textural Differences Induced by Water and Furnace Cooling in Commercially Pure Zr Annealed in the α + β Region. Metals and Materials International, 2018, 24, 673-680.	1.8	12
58	Microstructural characteristics of as-forged and β -air-cooled Zr–2.5Nb alloy. Transactions of Nonferrous Metals Society of China, 2018, 28, 1321-1328.	1.7	8
59	Homogenization and Growth Behavior of Second-Phase Particles in a Deformed Zr–Sn–Nb–Fe–Cu–Si–O Alloy. Metals, 2018, 8, 759.	1.0	16
60	EBSD Study of Microstructural and Textural Changes of Hot-Rolled Ti–6Al–4V Sheet After Annealing at 800°C. Acta Metallurgica Sinica (English Letters), 2018, 31, 1215-1223.	1.5	28
61	Deformation mode-determined misorientation and microstructural characteristics in rolled pure Zr sheet. Science China Technological Sciences, 2018, 61, 1346-1352.	2.0	13
62	Evolution of gradient microstructure in an extruded AZ31 rod during torsion and annealing and its effects on mechanical properties. Materials Science & Engineering A: Structural Materials: Properties, Microstructure and Processing, 2017, 689, 78-88.	2.6	47
63	Microstructure and dry sliding wear behavior of laser clad AlCrNiSiTi multi-principal element alloy coatings. Rare Metals, 2017, 36, 562-568.	3.6	25
64	Influence of Torsion Route on the Microstructure and Mechanical Properties of Extruded AZ31 Rods. Advanced Engineering Materials, 2017, 19, 1700267.	1.6	14
65	EBSD analysis on restoration mechanism of as-extruded AA2099 Al-Li alloy after various thermomechanical processes. Materials Chemistry and Physics, 2017, 191, 99-105.	2.0	20
66	Bimodal plate structures induced by pulsed laser in duplex-phase Zr alloy. Science China Technological Sciences, 2017, 60, 587-592.	2.0	7
67	Annealing behavior of gradient structured copper and its effect on mechanical properties. Materials Science & Engineering A: Structural Materials: Properties, Microstructure and Processing, 2017, 702, 331-342.	2.6	31
68	Characterization of microstructure and hardness of a Zr-2.5Nb alloy surface-treated by pulsed laser. Materials Chemistry and Physics, 2017, 198, 303-309.	2.0	28
69	α→β Transformation characteristics revealed by pulsed laser-induced non-equilibrium microstructures in duplex-phase Zr alloy. Science China Technological Sciences, 2017, 60, 1255-1262.	2.0	34
70	On the microstructure and mechanical property of as-extruded Mg-Gd-Y-Zn alloy with Sr addition. Materials Science & Engineering A: Structural Materials: Properties, Microstructure and Processing, 2017, 679, 183-192.	2.6	13
71	Microstructure and corrosion behavior of a Zr-Sn-Nb-Fe-Cu-O alloy fabricated by $\hat{I} \pm \hat{I}^2$ quenching processing. IOP Conference Series: Materials Science and Engineering, 2017, 182, 012019.	0.3	1
72	Surface Modification of Aluminized Cu-10Fe Alloy by High Current Pulsed Electron Beam. Materials Research, 2017, 20, 96-101.	0.6	12

#	Article	IF	CITATIONS
73	Influence of Electron Beam Irradiation on Surface Roughness of Commercially AISI 5140 Steel. Materials Transactions, 2017, 58, 1519-1523.	0.4	5
74	Correlation between localized plastic deformation and localized corrosion in AA2099 aluminumâ€lithium alloy. Surface and Interface Analysis, 2016, 48, 838-842.	0.8	21
75	Evolution of microstructure and grain boundary character distribution of a tin bronze annealed at different temperatures. Materials Characterization, 2016, 114, 204-210.	1.9	38
76	Investigation of microstructures of laser surface-treated Zr702 sheet using electron channeling contrast imaging and electron backscatter diffraction techniques. Surface and Coatings Technology, 2016, 296, 13-19.	2.2	7
77	Texture evolution and microstructural thermal stability of as-extruded AA2099 during hot deformation. Materials Science & Engineering A: Structural Materials: Properties, Microstructure and Processing, 2016, 675, 431-436.	2.6	14
78	Microstructural, textural and hardness evolution of commercially pure Zr surface-treated by high current pulsed electron beam. Applied Surface Science, 2016, 390, 430-434.	3.1	27
79	Preparation and characterization of Mg alloy rods with gradient microstructure by torsion deformation. Metals and Materials International, 2016, 22, 887-896.	1.8	24
80	Activating profuse pyramidal slips in magnesium alloys via raising strain rate to dynamic level. Journal of Alloys and Compounds, 2016, 688, 149-152.	2.8	20
81	Microstructures and Mechanical Properties of Commercial Hotâ€Extruded Copper Processed by Torsion Deformation. Advanced Engineering Materials, 2016, 18, 1738-1746.	1.6	13
82	Concurrent inheritance of microstructure and texture after slow β→α cooling of commercially pure Zr. Science China Technological Sciences, 2016, 59, 1771-1776.	2.0	9
83	Electron backscatter diffraction investigation of duplex-phase microstructure in a forged Zr-2.5Nb alloy. Science China Technological Sciences, 2016, 59, 673-679.	2.0	14
84	Microstructural changes of Zr702 induced by pulsed laser surface treatment. Applied Surface Science, 2016, 364, 61-68.	3.1	39
85	Microstructure and Liquid Phase Separation of CuCr Alloys Treated by High Current Pulsed Electron Beam. Materials Research, 2015, 18, 34-39.	0.6	6
86	Microstructural and textural evolution of commercially pure Zr sheet rolled at room and liquid nitrogen temperatures. Materials and Design, 2015, 85, 296-308.	3.3	73
87	Evolution of surface microstructure of Cu-50Cr alloy treated by high current pulsed electron beam. Science China Technological Sciences, 2015, 58, 462-469.	2.0	22
88	Surface modification of Cu–25Cr alloy induced by high current pulsed electron beam. Transactions of Nonferrous Metals Society of China, 2015, 25, 1935-1943.	1.7	18
89	A special twin relationship or a common Burgers misorientation between α plates after β quenching in Zr alloy?. Materials Characterization, 2015, 104, 61-65.	1.9	29
90	Microstructural characteristics of a commercially pure Zr treated by pulsed laser at different powers. Materials Characterization, 2015, 110, 25-32.	1.9	19

#	Article	IF	CITATIONS
91	Effects of heating rates and alloying elements (Sn, Cu and Cr) on the α → α + β phase transformation of Zr–Sn–Nb–Fe–(Cu, Cr) alloys. Journal of Nuclear Materials, 2014, 453, 269-274.	1.3	15
92	Experimental observation of 12 α variants inherited from one β grain in a Zr alloy. Journal of Nuclear Materials, 2013, 440, 377-381.	1.3	41
93	Twinning during recrystallization cooling in α-Zr alloy. Materials Science & Engineering A: Structural Materials: Properties, Microstructure and Processing, 2013, 576, 320-325.	2.6	22
94	Effect of predeformation on microstructural evolution of a Zr alloy during 550–700°C aging after β quenching. Acta Materialia, 2013, 61, 3099-3109.	3.8	53
95	Compression deformation behavior of Zr–1Sn–0.3Nb alloy with different initial orientations at 650 °C. Materials & Design, 2013, 52, 1065-1070.	5.1	29
96	Precise determination of the α→α+β phase transformation temperature of Zr-1.0Sn-0.3Nb-0.3Fe alloy. Science China Technological Sciences, 2013, 56, 60-65.	2.0	7
97	Formation and evolution of adiabatic shear bands in zirconium alloy impacted by split Hopkinson pressure bar. Journal of Nuclear Materials, 2013, 437, 380-388.	1.3	11
98	HETEROGENEOUS MICROSTRUCTURE AND TEXTURE EVOLUTION DURING FABRICATION OF ZrSnNb ZIRCONIUM ALLOY SHEETS. Jinshu Xuebao/Acta Metallurgica Sinica, 2013, 48, 393-400.	0.3	8
99	Twinning during β→α slow cooling in a zirconium alloy. Scripta Materialia, 2012, 67, 716-719.	2.6	20
100	Characterization of adiabatic shear bands in the zirconium alloy impacted by split Hopkinson pressure bar at a strain rate of 6000sâ°1. Materials Science & Engineering A: Structural Materials: Properties, Microstructure and Processing, 2012, 558, 517-524.	2.6	21
101	Effect of cooling rate on β →α transformation during quenching of a Zr-0.85Sn-0.4Nb-0.4Fe-0.1Cr-0.05Cu alloy. Science China Technological Sciences, 2012, 55, 2960-2964.	2.0	26
102	Growth behavior study of second phase particles in a Zr–Sn–Nb–Fe–Cr–Cu alloy. Journal of Nuclear Materials, 2012, 423, 127-131.	1.3	26
103	Study of precipitate evolution and recrystallization of β-quenched Zr–Sn–Nb–Fe–Cr–Cu alloy during aging. Journal of Nuclear Materials, 2012, 427, 274-281.	1.3	29
104	EFFECT OF PRE-DEFORMATION ON GRAINS AND PRECIPITATES OF Zr-Sn-Nb ALLOY DURING AGING. Jinshu Xuebao/Acta Metallurgica Sinica, 2012, 48, 107.	0.3	3
105	Microstructural Modification of Brush-Plated Nanocrystalline Cr by High Current Pulsed Electron Beam Irradiation. Journal of Nano Research, 0, 41, 87-95.	0.8	7